



## **On periodic boundary conditions in Variationally Consistent Homogenisation of beams and plates**

Downloaded from: <https://research.chalmers.se>, 2024-04-18 23:07 UTC

Citation for the original published paper (version of record):

Sciegaj, A., Grassl, P., Larsson, F. et al (2019). On periodic boundary conditions in Variationally Consistent Homogenisation of beams and plates. Proceedings of the 32nd Nordic Seminar on Computational Mechanics

N.B. When citing this work, cite the original published paper.

# On periodic boundary conditions in Variationally Consistent Homogenisation of beams and plates

Adam Sciegaj<sup>1,2</sup>, Peter Grassl<sup>3</sup>, Fredrik Larsson<sup>1</sup>, Karin Lundgren<sup>2</sup> and Kenneth Runesson<sup>1</sup>

<sup>(1)</sup> Department of Industrial and Materials Science, Chalmers University of Technology, Sweden, adam.sciegaj@chalmers.se, fredrik.larsson@chalmers.se, kenneth.runesson@chalmers.se

<sup>(2)</sup> Department of Architecture and Civil Engineering, Chalmers University of Technology, Sweden, karin.lundgren@chalmers.se

<sup>(3)</sup> School of Engineering, University of Glasgow, United Kingdom, peter.grassl@glasgow.ac.uk

**Summary.** A computationally efficient strategy to prescribe periodic boundary conditions on three-dimensional Representative Volume Elements (RVEs) is outlined. In particular, the cases of having an Euler-Bernoulli beam and a Kirchhoff-Love plate problem at the macroscale are considered within a computational homogenisation framework. Special solid elements for the boundary region of the periodic mesh have been developed, in which some of the degrees of freedom depend on those of their periodic counterparts, the macroscopic data and the size of the RVE.

*Key words:* periodicity, computational homogenisation, beam, plate, multiscale

## Introduction

Computational Multiscale Modelling (CMM), specifically the FE<sup>2</sup> method, is suitable for analysis of large-scale reinforced concrete structures, such as e.g. bridges. Detailed results such as crack widths and crack patterns can be efficiently obtained for large structures, where conventional single-scale finite element analyses would be impractical. In the FE<sup>2</sup> method, the large-scale effective response is obtained from computational homogenisation of the response of Representative Volume Elements (RVEs), which are located at the integration points. The macroscopic fields are prescribed on the RVEs via suitable boundary conditions, and the response is homogenised (averaged) to produce a macroscopic quantity, cf. [1]. In order to increase computational efficiency of the model, the large-scale structure can often be modelled with plate/shell elements, while the detailed subscale response of the material is best described with three-dimensional RVE models. In this work, we outline the main formulation of the large-scale and subscale problems for macroscopic Euler-Bernoulli beams and Kirchhoff-Love plates. A computationally efficient way of prescribing the macroscopic fields via periodic boundary conditions at the subscale, using special tetrahedral elements developed in this study, is presented.

## Large-scale problem

The large-scale problem for an *Euler-Bernoulli beam*, which occupies region  $[0, L]$  and is subjected to bending around the y-axis, can be expressed in the weak form as follows:

$$\int_0^L \bar{N} \frac{\partial \delta \bar{u}}{\partial x} dx = [N_p \delta \bar{u}]_0^L + \int_0^L b \delta \bar{u} dx, \quad (1)$$

$$\int_0^L \bar{M} \frac{\partial^2 \delta \bar{w}}{\partial x^2} dx = \left[ M_p \frac{\partial \delta \bar{w}}{\partial x} \right]_0^L - [V_p \delta \bar{w}]_0^L - \int_0^L q \delta \bar{w} dx, \quad (2)$$

for suitable test functions  $\delta\bar{u}$  and  $\delta\bar{w}$ . Here,  $\bar{u}$  and  $\bar{w}$  are the macroscopic displacements in x- and z-directions, while  $b$  and  $q$  are the corresponding distributed loads. The forces  $N_p$ ,  $V_p$ , and  $M_p$  are the prescribed normal forces, shear forces and bending moments, respectively. The effective normal force  $\bar{N}$  and effective bending moment  $\bar{M}$  are obtained from computational homogenisation upon solution of the pertinent RVE problem as

$$\bar{N} = \frac{1}{|L_\square|} \int_{\Omega_\square} \sigma_{xx} \, d\Omega, \quad \bar{M} = \frac{1}{|L_\square|} \int_{\Omega_\square} z \sigma_{xx} \, d\Omega, \quad (3)$$

where  $\sigma_{xx}$  is the normal stress in x-direction,  $L_\square$  is the length of the RVE in the x-direction, and  $\Omega_\square$  is the volume of the representative volume element.

For a *Kirchhoff-Love plate* occupying region  $\Omega$  with boundary  $\partial\Omega = \Gamma$ , the corresponding large-scale problem can be expressed in the weak form as follows:

$$\int_{\Omega} \bar{\mathbf{N}} : [\delta\bar{\mathbf{u}} \otimes \nabla] \, d\Omega = \int_{\Gamma} \mathbf{N}_p \cdot \delta\bar{\mathbf{u}} \, d\Gamma + \int_{\Omega} \mathbf{b} \cdot \delta\bar{\mathbf{u}} \, d\Omega, \quad (4)$$

$$\int_{\Omega} \bar{\mathbf{M}} : [\delta\bar{w} \otimes \nabla^*] \, d\Omega = \int_{\Gamma} V_i^K \delta\bar{w} \, d\Gamma - \int_{\Gamma} M_{ii} \frac{\partial \delta\bar{w}}{\partial i} \, d\Gamma + \int_{\Omega} q \delta\bar{w} \, d\Omega, \quad (5)$$

for suitable test functions  $\delta\bar{\mathbf{u}}$  and  $\delta\bar{w}$ . Here,  $\nabla$  and  $\nabla^*$  are the differential and curvature operators. The macroscopic fields  $\bar{\mathbf{u}}^T = [\bar{u} \, \bar{v}]$  and  $\bar{w}$  are the in- and out-of-plane displacement fields, while  $\mathbf{b}$  and  $q$  are the corresponding distributed loads. The forces  $\mathbf{N}_p$ ,  $V_i^K$  are the prescribed boundary normal and Kirchhoff forces, while  $M_{ii}$  is the prescribed boundary bending moment. The effective membrane forces,  $\bar{\mathbf{N}}$ , and bending moments,  $\bar{\mathbf{M}}$ , can be obtained upon solving the RVE problem as

$$\bar{\mathbf{N}} = \frac{1}{|A_\square|} \int_{\Omega_\square} \hat{\boldsymbol{\sigma}} \, d\Omega, \quad \bar{\mathbf{M}} = \frac{1}{|A_\square|} \int_{\Omega_\square} z \hat{\boldsymbol{\sigma}} \, d\Omega, \quad (6)$$

where  $\hat{\boldsymbol{\sigma}}$  denotes the in-plane projection of the Cauchy stress and  $A_\square$  is the area of the RVE in the xy-plane.

### Subscale problem with periodic boundary conditions

The weak form of the three-dimensional boundary value problem on the RVE is defined in terms of finding the unknown displacement field  $\mathbf{u}^T = [u \, v \, w]$  from the momentum equilibrium relation

$$\int_{\Omega_\square} \boldsymbol{\sigma} : [\delta\mathbf{u} \otimes \nabla] \, d\Omega = \int_{\Gamma_\square} \hat{\mathbf{t}} \cdot \delta\mathbf{u} \, d\Gamma, \quad (7)$$

with suitable boundary conditions and pertinent test functions  $\delta\mathbf{u}$ . In this relation, the RVE is defined within the region  $\Omega_\square$  and is subjected to tractions  $\hat{\mathbf{t}}$  on its boundary  $\partial\Omega_\square = \Gamma_\square$ . In this work, we consider periodic boundary conditions, which state that the fluctuation part of the total fields are equal at both boundaries of the RVE. To this end, we define the image (plus) side and the mirror (minus) side of the representative volume element. The difference in deformation at these two boundaries is simply governed by the (gradients of) macroscopic fields. For the *Euler-Bernoulli beam* we have the following relations linking the macro- and microfields:

$$u^+ - u^- = \left[ \frac{\partial \bar{u}}{\partial x} - z \frac{\partial^2 \bar{w}}{\partial x^2} \right] [x^+ - x^-], \quad (8)$$

$$w^+ - w^- = \frac{\partial \bar{w}}{\partial x} [x^+ - x^-], \quad (9)$$

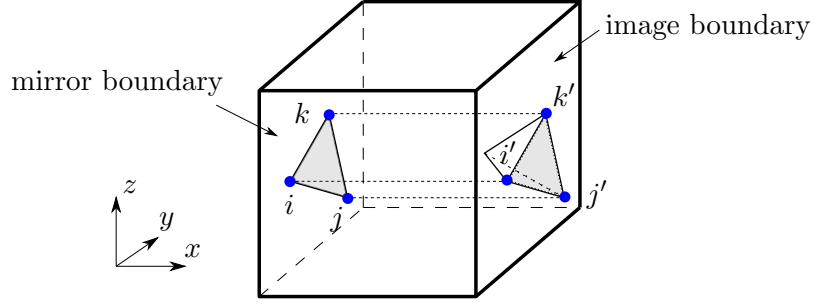


Figure 1. Boundary tetrahedral finite element in a cube RVE with periodicity in x-direction. Nodes  $i'$ ,  $j'$ , and  $k'$  are replaced by their periodic counterparts  $i$ ,  $j$ ,  $k$ .

where  $x^+$  and  $x^-$  are the x-coordinates of the image and mirror boundaries, respectively. For the *Kirchhoff-Love plate* at the macroscale the corresponding relations are:

$$u^+ - u^- = \left[ \frac{\partial \bar{u}}{\partial x} - z \frac{\partial^2 \bar{w}}{\partial x^2} \right] [x^+ - x^-] + \left[ \frac{\partial \bar{u}}{\partial y} - z \frac{\partial^2 \bar{w}}{\partial x \partial y} \right] [y^+ - y^-], \quad (10)$$

$$v^+ - v^- = \left[ \frac{\partial \bar{v}}{\partial x} - z \frac{\partial^2 \bar{w}}{\partial x \partial y} \right] [x^+ - x^-] + \left[ \frac{\partial \bar{v}}{\partial y} - z \frac{\partial^2 \bar{w}}{\partial y^2} \right] [y^+ - y^-], \quad (11)$$

$$w^+ - w^- = \frac{\partial \bar{w}}{\partial x} [x^+ - x^-] + \frac{\partial \bar{w}}{\partial y} [y^+ - y^-]. \quad (12)$$

The differences  $x^+ - x^-$  and  $y^+ - y^-$  represent the distances between the image and mirror boundaries normal to  $x$  and  $y$  directions. In the usual case of a cuboid RVE, these simply translate to the lengths in x- and y-direction, respectively.

### Modified boundary tetrahedral finite element

In order to resolve relations (8)–(12) in the RVE model, a new element was developed and implemented in the open-source code OOFEM [4]. The element, inspired by similar periodic formulation from [2] and [3], is based on the classical tetrahedral element with linear shape functions and is intended to represent part of the image boundary of the RVE, cf. Figure 1.

The user defines the boundary element using only the corresponding nodes at the mirror boundary, the direction of periodicity and the size of the RVE. Additionally, one control node is defined for the model and is also used in the boundary element definition. The control node is intended to contain the macroscopic information about the effective fields within its degrees of freedom. Depending on the macroscopic problem (Euler-Bernoulli beam or Kirchhoff-Love plate), the control node has either 3 or 10 degrees of freedom - the partial derivatives in relations (8)–(12). Using these relations, it is possible to express the unknown degrees of freedom of any boundary element at the image boundary as function of the degrees of freedom of the corresponding nodes at mirror boundary and the macroscopic information from the control node, i.e.

$$\mathbf{u}' = \mathbf{T}\mathbf{u}, \quad (13)$$

where  $\mathbf{u}'$  is the vector containing the displacement degrees of freedom at the image boundary, while  $\mathbf{u}$  contains the displacement degrees of freedom of the corresponding nodes at the mirror boundary as well as the degrees of freedom of the control node. The matrix  $\mathbf{T}$  is basically a unit matrix expanded by the corresponding entries from Equations (8)–(12). At any iteration step, after evaluating the element deformations  $\mathbf{u}'$  according to Equation (13), the element stiffness matrix  $\mathbf{K}'$  and internal force vector  $\mathbf{f}'_{\text{int}}$  can be computed in the usual fashion. In order to transfer

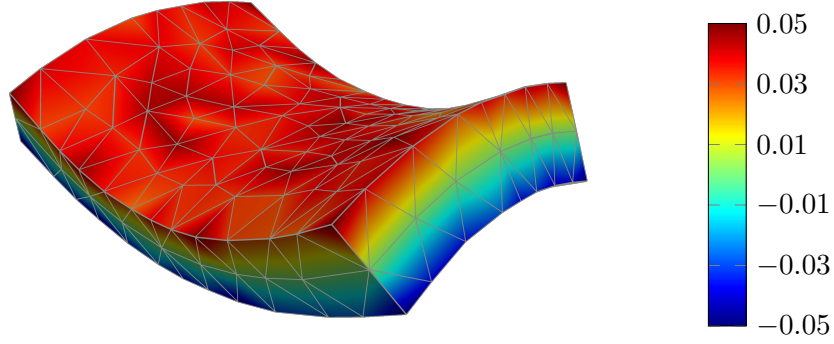


Figure 2. Contour plot of the strain  $\varepsilon_{yy}$  in a plate RVE subjected to macroscopic curvatures  $\partial^2 \bar{w}/\partial x^2 = 1$ ,  $\partial^2 \bar{w}/\partial y^2 = -1$

back to the mirror boundary and continue with the assembly, we use the following relations:

$$\mathbf{K} = \mathbf{T}^T \mathbf{K}' \mathbf{T}, \quad \mathbf{f}_{\text{int}} = \mathbf{T}^T \mathbf{f}'_{\text{int}}. \quad (14)$$

### Example response

In order to illustrate the method, a sample linear elastic RVE in shape of a cuboid with sizes  $L_x = 0.6$  m,  $L_y = 0.4$  m and  $L_z = 0.1$  m was considered. A periodic tetrahedral mesh was created following the method described in [2] and [3]. Subsequently, all elements with nodes at the image boundaries were replaced by the corresponding modified boundary tetrahedra. Macroscopic curvatures  $\partial^2 \bar{w}/\partial x^2 = 1$ ,  $\partial^2 \bar{w}/\partial y^2 = -1$  were imposed on the RVE by prescribing them as boundary conditions in the corresponding degrees of freedom of the control node. The deformed shape and a contour plot of the strain  $\varepsilon_{yy}$  can be seen in Figure 2. It is noteworthy that the obtained reaction forces in the control node are the effective forces (moments), that can be used directly in the FE<sup>2</sup> scheme.

### Conclusions

We proposed new boundary tetrahedral elements, which make it possible to impose an arbitrary combination of macroscopic in-plane strains, slopes and curvatures as periodic boundary conditions on the RVE. This is a necessary step to apply the FE<sup>2</sup> procedure to large-scale structures modelled with beam and plate/shell elements.

### References

- [1] F. Larsson, K. Runesson and F. Su. Variationally consistent computational homogenization of transient heat flow. *International Journal for Numerical Methods in Engineering*, 81: 1659–1686, 2010.
- [2] I. Athanasiadis, S. J. Wheeler and P. Grassl. Hydro-mechanical network modelling of particulate composites. *International Journal of Solids and Structures*, 130–131: 49–60, 2018.
- [3] P. Grassl and M. Jirásek. Meso-scale approach to modelling the fracture process zone of concrete subjected to uniaxial tension. *International Journal of Solids and Structures*, 47: 957–968, 2010.
- [4] B. Patzák. OOFEM - an object-oriented simulation tool for advanced modeling of materials and structures. *Acta Polytechnica*, 52(6):59–66, 2012